

Hysteresis and Lubrication in Shear Thickening of Cornstarch Suspensions

Clarence E. Chu, Joel A. Groman, Hannah L. Sieber, and James G. Miller

Department of Physics, Washington University, St. Louis, Mo. 63130

Ruth J. Okamoto

Department of Mechanical Engineering and Materials Science,

Washington University, St. Louis, Mo. 63130

Jonathan I. Katz*

Department of Physics, Washington University, St. Louis, Mo. 63130 and

McDonnell Center for the Space Sciences,

Washington University, St. Louis, Mo. 63130^a

(Dated: May 29, 2014)

Abstract

Aqueous and brine suspensions of cornstarch show striking discontinuous shear thickening. We have found that a suspension shear-thickened throughout may remain in the jammed thickened state as the strain rate is reduced, but an unjamming front may propagate from any unjammed regions. Transient shear thickening is observed at strain rates below the thickening threshold, and above it the stress fluctuates. The jammed shear-thickened state may persist to low strain rate, with stresses resembling sliding friction and effective viscosity inversely proportional to the strain rate. At the thickening threshold fluid pressure depins the suspension's contact lines on solid boundaries, so that it slides, shears, dilates and jams. In oil suspensions lubrication and complete wetting of confining surfaces eliminate contact line forces and prevent jamming and shear thickening, as does addition of immiscible liquid surfactant to brine suspensions. Starch suspensions in glycerin-water solutions, viscous but incompletely wetting, have intermediate properties.

PACS numbers: 47.55.dk,47.55.Kf,47.55.np,47.57.E-,47.57.Qk

INTRODUCTION

Aqueous and brine suspensions of cornstarch have long been known [1–5] to show the dramatic property of discontinuous shear thickening (DST). Cornstarch is a complex biogenic substance consisting of polydisperse grains with mean diameter $\approx 14\mu$ and blocky irregular shapes. The ready observation of DST in cornstarch suspensions over a broad range of starch fractions and conditions illustrates the robustness and universality of the phenomenon.

Shear thickening interferes with some industrial processes [3] but may be useful to absorb mechanical energy [6, 7] or to suppress hydrodynamic instability [8]. Thickened starch suspensions show quasi-solid behavior: rapid stirring produces tensile fracture and uncovers the bottom of a shallow container. In contrast, starch suspensions in nonpolar fluids, such as oils, benzene and CCl_4 , are unremarkable shear thinning fluids [1, 9]. An explanation of shear thickening of starch suspensions in water and brine must also explain its absence in starch suspensions in oil.

Cornstarch occupies an intermediate regime between colloids and macroscopic particles. Interactions [10] that lead to non-Newtonian properties of colloidal suspensions are insignificant. Starch grains are small enough to form suspensions, yet large enough that these suspensions are non-Brownian: the Péclet number at the DST threshold $\text{Pe} \equiv \frac{a^2\dot{\gamma}}{D} = \frac{6\pi\eta_f a^3\dot{\gamma}}{k_B T} \gtrsim 2000$, where $a \approx 7\mu$ is the mean particle radius, the strain rate $\dot{\gamma} = \dot{\gamma}_c \gtrsim 2/\text{s}$ where $\dot{\gamma}_c$ is the critical strain rate for shear thickening, η_f the dynamic viscosity of the solvent and D the Brownian diffusivity.

HYSTERESIS

The richness of the rheological properties of cornstarch suspensions includes remarkable hysteresis [11–14]. Fig. 1 shows the behavior of suspensions of cornstarch in density-matched CsCl brine. The strain rate was first stepped up from low values into the shear-thickened regime, and then stepped down. When shear is imposed between a rotating cone and a static flat plate the strain rate is homogeneous. Hysteresis is evident; once the suspension has jammed in the shear-thickened state, even a low strain rate is sufficient to keep it jammed (Fig. 1(a)). We infer (but cannot directly observe) that the entire suspension jams. The normal stress imposed by the rheometer to maintain a constant gap width is small and

negative [15] in the unthickened state but large, positive, and roughly constant once the suspension has thickened, even as $\dot{\gamma}$ is stepped down below $\dot{\gamma}_c$. We attribute this to the large normal stress and static friction between grains maintaining the jammed state against the shear stress.

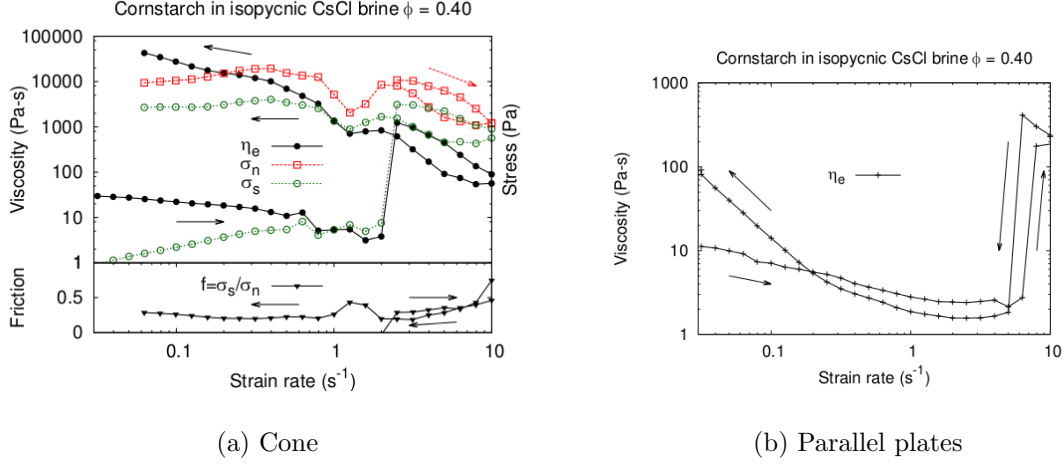


FIG. 1: Rheology of suspensions of cornstarch (starch fraction $\phi = 0.40$) in isopycnic (53.5%) CsCl aqueous brine. The strain rate was increased from 0.03/s to 10/s, and then decreased (directions shown with arrows) in discrete steps; each point represents a 60 s measurement at constant strain rate. Lines guide the eye between data points. (a) Homogeneous strain rate in conical (2°) geometry. The normal stress σ_n is small and negative ($\simeq -200$ Pa, nearly independent of strain rate; not shown), attributable to meniscus tension, until DST, but then becomes large, positive and very roughly independent of strain rate. Even low strain rates are sufficient to maintain the starch grains in their jammed state. The shear stress σ_s follows a sigmoidal curve [14] as the strain rate is increased, but remains high, like σ_n , even as the strain rate is reduced below $\dot{\gamma}_c$. Their ratio, an effective sliding friction coefficient [16], $f \equiv \sigma_s/\sigma_n \approx 0.3$. The effective viscosity $\eta_e \equiv \sigma_s/\dot{\gamma} \propto \dot{\gamma}^{-1}$ in the shear-thickened regime. (b) In parallel plate geometry (0.7 mm) the strain rate varies from zero on the axis to its maximal value ($\dot{\gamma}$, shown) at the periphery. Hysteresis is minimal; the suspension unjams as the strain rate is reduced. The larger value of $\dot{\gamma}_c$ may also be attributed to an unjamming front propagating from regions of lower $\dot{\gamma}$ near the axis. [Color on-line.]

In contrast, in parallel plate geometry the suspension thickened at $\dot{\gamma}_c \approx 6\text{--}8/\text{s}$ and unthickened when $\dot{\gamma}$ was reduced slightly below this value, as shown in Fig. 1(b). This suggests that an unjamming front propagated from unjammed suspension near the rotation axis where $\dot{\gamma} < \dot{\gamma}_c$ into jammed material, as granules on the front became free to reorient themselves and force chains were disrupted. Analogous behavior is found for suspensions of BiOCl [17] in which contact with fluid material initiates a liquifaction front that propagates into jammed quasi-solid material, and similar phenomena may be involved in mudslides.

Even at steady strain rates, hysteresis is observed near the DST threshold (Fig. 2). For $\dot{\gamma}$

slightly below $\dot{\gamma}_c$ (but not for yet smaller $\dot{\gamma}$) each increment in $\dot{\gamma}$ produces an initial thickening followed by rapid relaxation into a steady and less viscous state. This may be explained as the disruption of transient force chains [18] by the shear flow when the stress is insufficient to maintain frictional contacts within force chains and between them and confining surfaces.

At and above the DST threshold (which is steep but not truly discontinuous; Fig. 2(b)) σ_s fluctuates with large amplitude, suggesting a quasi-solid jammed suspension, maintained by a larger normal stress σ_n , that intermittently slips, fractures, or partially jams and unjams. These fluctuations might suggest stick-slip friction, but this is not consistent with the steady σ_s when $\dot{\gamma}$ is reduced but the suspension remains jammed in conical geometry ($\dot{\gamma} = 0.316/\text{s}$ in Fig. 2(a)). The fact that the fractional fluctuation amplitude is greater for parallel plates also suggests a contribution from fluctuation of a jammed/unjammed boundary at small radius, rather than it being entirely a stick-slip phenomenon independent of the specific geometry.

This fluctuating stress in the DST regime resembles that observed for colloids [19] at much higher strain rates. In experiments with larger ($5.8\ \mu$) non-Brownian particles (expected to be in the same regime as cornstarch), in which stress was the control parameter, a fluctuating $\dot{\gamma}$ was observed [20]. However, this may be explained by a multivalued $\dot{\gamma}(\sigma_s)$ and mechanical relaxation between its two values rather than by intrinsic hysteresis.

Fluctuating stress cannot be explained as a consequence of statistical fluctuations in the number of independent force chains: A simple estimate, using Hertzian contact theory, shows that for a mean stress σ_n applied over an area A to a layer of thickness h of grains of Young's modulus E [21], radius a , and radius of curvature at their contacts r_{curv} , the number of force chains carrying the load

$$n_{chain} \simeq \frac{A}{a^2} \left(\frac{\sigma_n}{E}\right)^{2/5} \left(\frac{h}{a}\right)^{3/5} \left(\frac{a}{r_{curv}}\right)^{1/5} \simeq 10^6 \left(\frac{a}{r_{curv}}\right)^{1/5} \gg 1. \quad (1)$$

Even jamming on the scale h would lead to $n_{block} \simeq A/h^2 \simeq 2000$ of independent blocks. The amplitude of the measured stress fluctuations implies that the entire jammed volume acts as a single solid body.

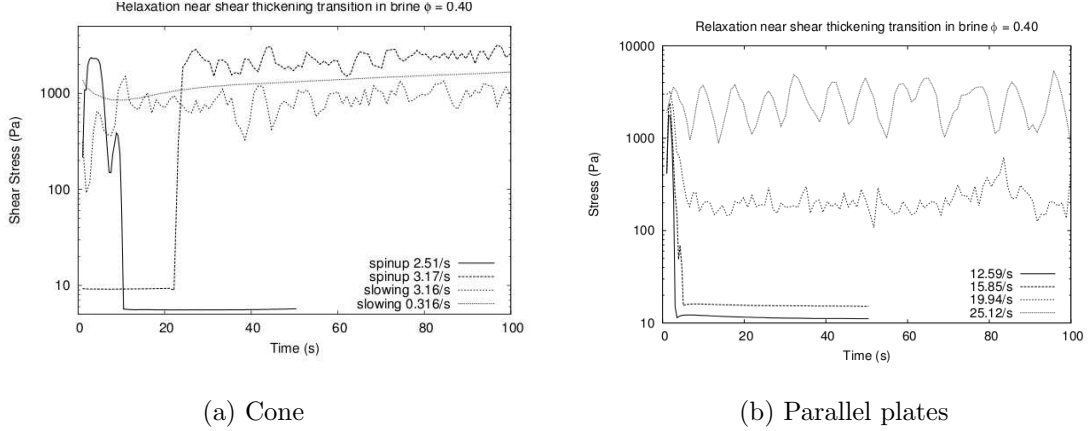


FIG. 2: Variations of shear stress σ_s with time at constant strain rate $\dot{\gamma}$ after stepping up (spinup) or down (slowing); (a) In conical geometry (2°) σ_s fluctuates in the jammed state after DST at $2.51/\text{s} < \dot{\gamma}_c < 3.17/\text{s}$; similar behavior was observed as $\dot{\gamma}$ was increased to $10/\text{s}$, and subsequently decreased. After slowing to $\dot{\gamma} \ll \dot{\gamma}_c$, σ_s was roughly unchanged but steady ($\dot{\gamma} = 0.316/\text{s}$ shown). (b) In parallel plate geometry ($\dot{\gamma}$ at rim, 0.5 mm) for $\dot{\gamma} < 10/\text{s}$ σ_s relaxes within 1 s to a new steady value with no indication of transient behavior (not shown). For slightly higher $\dot{\gamma} \lesssim \dot{\gamma}_c \approx 20/\text{s}$ there is transient thickening, followed by relaxation over a few seconds into a less viscous quicksand-like state. For $\dot{\gamma} \gtrsim \dot{\gamma}_c$ the suspension shear thickens as granules jam and unjam and σ_s fluctuates with large amplitude rather than settling to a steady value. This behavior continues to strain rates several times higher than $\dot{\gamma}_c$ (as high as it has been possible to shear the suspension without expelling it centrifugally).

SURFACES AND CONFINEMENT

The values of $\dot{\gamma}_c$ and of the effective viscosity $\eta_e(\dot{\gamma}_c)$ in the shear-thickened state require explanation. The dimensional parameters a and ν_f define a dimensional strain rate $\dot{\Gamma} \equiv \nu_f/a^2 \approx 2 \times 10^4/\text{s} \gg \dot{\gamma}_c$, where ν_f is the kinematic viscosity of the solvent; substitution of the suspension viscosity for ν_f would multiply Pe and ν_f/a^2 by an additional large factor. No dimensionless groups exist to multiply or divide $\dot{\Gamma}$ to bring it into agreement with $\dot{\gamma}_c$.

An additional physical effect and dimensional parameter are required. The introduction of a surface energy γ permits defining a new dimensionless parameter, the surfuidity:

$$\text{Su} \equiv \frac{\gamma s}{\rho \nu_f^2}, \quad (2)$$

where s is a characteristic length, such as the particle radius a or layer thickness h . Su measures the comparative importance of surface and viscous forces and is equivalent to the Reynolds number of a partially wetted particle or flow acted upon only by surface forces

at its contact line and by viscosity. When two surfaces are brought together the sign of γ is significant: if the fluid reduces the interfacial energy then $\gamma < 0$ and a lubricating layer persists, but if $\gamma > 0$ surface forces expel this layer, bringing the solids into dry contact. If $s = a$ then for cornstarch in water or brine $|\text{Su}| \approx 200$, but in olive oil $|\text{Su}| \approx 0.06$ (taking $|\gamma| = 50$ dyne/cm, a representative value for molecular liquids). Surface energies are important for low viscosity solvents, but viscosity may be sufficient to maintain lubrication by more viscous solvents.

DST of aqueous and brine starch suspensions is attributed [4, 6, 16, 22, 23] to confinement of the grains by surface tension, in analogy to the shear thickening of larger particles confined by solid walls. During shear thickening the suspension has a “dry” or “rough” appearance [6, 22–26] indicative of particles pushed through the surface of the solvent as a consequence of shear dilatancy [27] (packed particles dilate when sheared because they are subject to too many constraints on displacement and rotation at unlubricated contacts to permit shear until some constraints are relieved by dilation). Surface tension acting on these particles explains the viscosity in the thickened state. It applies a confining stress $\sigma_c = O(\gamma/a) = O(10^4 \text{ Pa})$ [22, 24] to the particles. Unjammed, particles are individually pushed back into the body of the fluid, but if they are jammed this confining compressive stress is applied to the entire particle network. This also holds (with γ the interfacial tension) if the suspension is immersed in an immiscible fluid, such as a brine suspension immersed in oil [8]. If there is no opposing momentum supplied by the walls or bottom of a container [28] then momentum conservation requires a balancing tension in the fluid [29]. The fluid tension may be sufficient to induce fracture or cavitation, as observed in a vigorously stirred suspension in an open vessel.

In the Coulomb-Mohr model of the strength of solids and of granular materials with unlubricated grain-grain static friction the shear strength is comparable to σ_c . The flow condition in the jammed state is that σ_s equal the strength, so that $\sigma_s \sim \sigma_c \sim \sigma_n$ ($\sigma_c \sim \sigma_n$ is required by the constrained rheometer geometry), independent of $\dot{\gamma}$. Sliding friction against confining surfaces [18], with an effective coefficient f , produces shear thickening with shear stress $\sigma_s = f\sigma_n = O(f\gamma/a)$ and effective viscosity $\eta_e \equiv \sigma_s/\dot{\gamma} \propto \dot{\gamma}^{-1}$ [22]. Fig. 1(a) shows this behavior both as $\dot{\gamma}$ increases and also as it decreases far below $\dot{\gamma}_c$; Hoffman [30, 31] found a similar result for $\dot{\gamma} > \dot{\gamma}_c$. The measured $\sigma_n \simeq 10^4 \text{ Pa}$ is comparable to γ/a for starch granules, as predicted. This model assumes that the differential motion of the rheometer

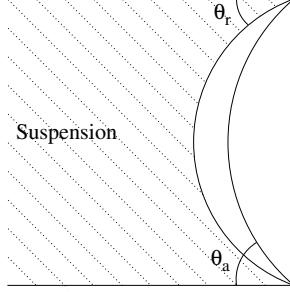


FIG. 3: Suspension confined between horizontal base plate and rotating parallel plate or shallow cone in a rheometer. Incipient dilation applies a force determined by the shear stress in the unjammed (shear-thinned) state to the three-phase contact line. If this force is sufficient to advance the contact line then the granules dilate and jam against the confining surfaces, producing discontinuous shear thickening.

surfaces is at least partly accommodated by shear (implying dilation) of the suspension, rather than entirely by surface slip. If it were entirely surface slip, the unsheared suspension would not be dilated or jammed, an inconsistency.

DST THRESHOLD

Surface tension may also explain the strain rate threshold $\dot{\gamma}_c$ of DST. A suspension that is free to expand does not undergo DST; confinement is required [4, 6, 16, 22, 23]. If at the edge of a gap of width h there is a free surface rather than additional fluid, as shown in Fig. 3, there is a confining meniscus stress on both granules and fluid $O(\gamma/h) = O(70 \text{ Pa})$, where $h \approx 0.07 \text{ cm}$ in most experiments, (the surface tension of CsCl brine is close to that of water [32]). This is also the source of the negative σ_n in the unstiffened state. Although much less than the internal stresses in the dilatant sheared state (because $h \gg a$), this stress is present even without strain.

A force chain [18] carrying a force F and making an angle θ to the normal and an azimuthal angle ϕ with respect to the flow direction applies a normal force $F \cos \theta$ and a tangential force $F \sin \theta \cos \phi$. Averaging over an isotropic distribution of force chains in $0 \leq \theta \leq \pi/2$ and $-\pi/2 \leq \phi \leq \pi/2$ (force chains cannot support tension) yields $\sigma_{s,chain} = \sigma_{n,chain}$. Sliding friction on the confining surfaces with coefficient f implies $\sigma_{s,chain} = \sigma_s = f\sigma_n$. Some

of the normal stress must be carried by a fluid pressure

$$P = \sigma_n - \sigma_{n,chain} = \sigma_s \left(\frac{1}{f} - 1 \right) \simeq 2\sigma_s \quad (3)$$

for $f \simeq 0.3$, as estimated in the fully shear-thickened state (Fig. 1(a)).

The maximum fluid pressure that can be sustained without moving the meniscus

$$P_{max} = \frac{2\gamma}{h}(\cos \theta_r - \cos \theta_a). \quad (4)$$

The receding and advancing contact angles θ_r and θ_a depend empirically on the surfaces and their condition, but in Fig. 1 $h = 0.07$ cm, the difference in cosines ≈ 0.15 [33] and $P_{max} \approx 20$ Pa. This value is consistent with the measured $\sigma_s \simeq 10$ Pa and inferred fluid $P \simeq 20$ Pa (Eq. 3) in the unthickened state at the threshold of DST shown in Fig. 1 and in [4]. Hoffman [10] found this stress to be independent of ν_f over three orders of magnitude, indicating that the thickening threshold is determined by surface tension and lubrication rather than by bulk properties of the solvent.

DST occurs in a steady flow with a free surface if (and only if) shear produces a dilational stress that moves the contact line between suspension, air and confining surface. The strain rate $\dot{\gamma}_c$ at the DST threshold is determined by P_{max} and the suspension viscosity (not that of the solvent) in the unstiffened state; stress and $\dot{\gamma}$, rather than ν_f , are the controlling parameters. At lower strain rates and stresses the meniscus deforms but the contact line does not move; the suspension does not slide on the confining surfaces and the granules do not jam. Once $P > P_{max}$ the suspension slides along the confining surfaces to accommodate dilation of the granules. With sufficient friction, dilation jams the granules against these surfaces [18, 34] and triggers DST. This is consistent with the observation [20] that wall slip is dramatically reduced or disappears when a suspension enters the dilatant regime.

OTHER SUSPENDING FLUIDS

We test these hypotheses by studying suspensions in fluids with different properties. Fig. 4 shows the rheology of suspensions of cornstarch in olive oil. It is not possible to match the density of oil to that of starch, but because the viscosity of olive oil is about 80 times that of water or brine [35, 36] and these suspensions are concentrated [37], sedimentation is slow.

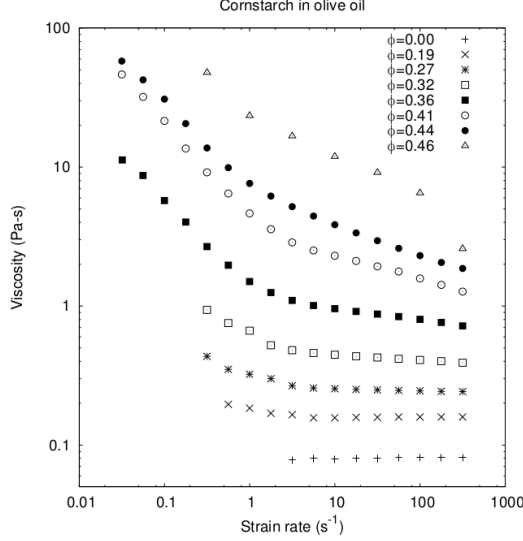


FIG. 4: Rheology of olive oil suspensions of cornstarch measured in a rotating 2° conical gap with 2 cm radius. Each point represents a steady state at constant strain rate. It was not possible to obtain reproducible data at very low strain rates for the most concentrated suspensions and or low torques (low strain rates for dilute suspensions). Shear thinning is evident, but not shear thickening. The normal stress σ_n remains small and negative, as for brine suspensions in the unthickened regime. One run at a starch volume fraction $\phi = 0.46$ provided evidence of a finite yield stress with divergent viscosity for $\dot{\gamma} < 0.01/\text{s}$, and such concentrated mixtures may resemble moist pastes rather than suspensions, but there was no evidence of a yield stress for $\phi \leq 0.44$.

There is no shear thickening, even at packing fractions ϕ at which shear thickening is evident in aqueous and brine suspensions [4], and no evidence of a yield stress [6, 16] sufficient to mask it. When increasing shear rate is followed, without stopping, by decreasing shear rate there is no evidence of hysteresis at levels of a few percent.

The absence of shear thickening and hysteresis in oil suspensions of starch is explained by the ability of oil to wet and spread along metal and glass surfaces, so that the particulate phase is effectively unconfined, as if it were in contact with a pool of suspension [4]. The sliding of starch grains along these surfaces is lubricated by films of oil wetting the surfaces. The viscosity of oil also makes it more effective in preventing frictional contacts between grains.

A glycerin/water (85%/15% by mass) solution is an intermediate between brine and olive oil as a solvent. The solvent viscosity equals that of olive oil, but its molecules are polar and its surface interactions similar to those of brine. Sedimentation of concentrated starch in glycerin/water is slow, as in oil [37]. Fig. 5(a) shows the results of measurements of

the effective viscosity of glycerin/water suspensions of cornstarch with and without added surfactant. These may be compared to the results for brine suspensions in Fig. 1. There is some shear thickening, but it is continuous, with little hysteresis, and by only a factor of about 5, rather than the 2–3 orders of magnitude of suspensions in brine. The surfactant does not qualitatively change its properties. The greater viscosity (Fig. 4) of oil suspensions in the shear thinning regime may be the result of greater clumping of granules [16], as occurs if they are more readily wetted by the polar solvent glycerin/water.

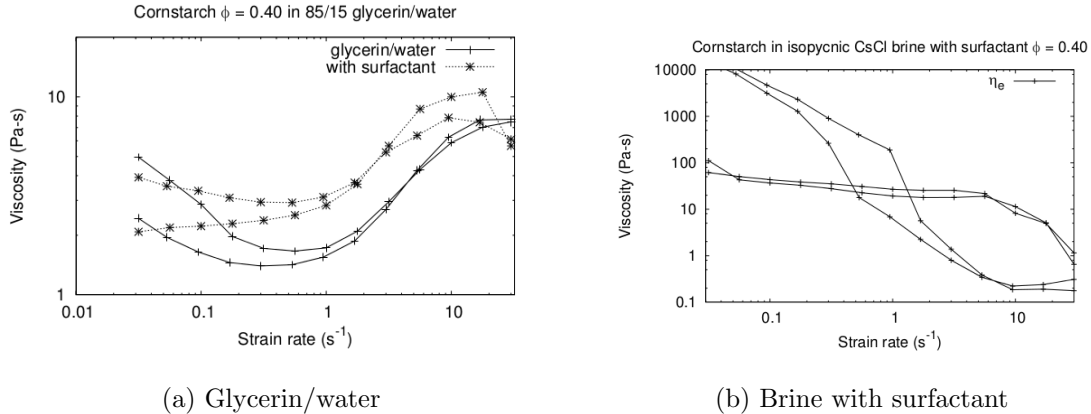


FIG. 5: Rheology of $\phi = 0.40$ suspensions of cornstarch in conical geometry in: (a) Glycerin/water solution with the same viscosity as olive oil, with and without miscible surfactant (dish detergent). (b) Isopycnic brine with an immiscible surfactant Triton X-100 (two runs). The glycerin/water suspension shear thickens, but much less than brine without surfactant (Fig. 1), continuously and without hysteresis. The viscous solvent interferes with jamming and DST, plausibly as a consequence of its greater lubricity. The surfactant has little effect, perhaps because the effect of viscosity is sufficient to lubricate contacts, without regard to surface interactions. In low viscosity brine the immiscible surfactant prevents shear thickening entirely, which we suggest is a consequence of its ability to wet and lubricate confining surfaces. There is little hysteresis but nominally identical samples have very different properties, perhaps as a result of differences in the distribution of buoyant surfactant.

The mild shear thickening of glycerin/water suspensions indicates that viscosity alone is insufficient to prevent shear thickening; wetting is also required. Because glycerin/water, like brine, incompletely wets metal and glass surfaces, contact line forces provide confinement and some shear thickening is observed. Its viscosity helps to maintain a lubricating film of fluid despite incomplete wetting, qualitatively explaining the observation that its shear thinning is modest in magnitude, gradual in onset and shows no hysteresis (Fig. 5(a)). The normal stress σ_n in the rheometer remains negative, as expected for a wetting fluid (Fig. 3 with $\theta_r = \theta_a = 0$). Shear dilation reduces gaps between grains and increases viscous coupling

among them, increasing the suspension viscosity, but is accommodated by sliding and the grains do not jam.

Fig. 5(b) shows the rheology of a starch suspension in isopycnic brine with a small quantity of surfactant (dish detergent) added. This surfactant is immiscible in the brine, so that it forms a third phase that wets and lubricates the confining surfaces in the same manner as oil. The particulate phase is effectively unconfined, precluding jamming and shear thickening. This result is the opposite of the effect of a secondary fluid whose addition turns a fluid suspension into an elastic gel [38]. We attribute the difference to the surfactant wetting the confining surfaces in our experiments.

DISCUSSION

In the DST state the grains in cornstarch suspensions in brine jam and shear between the confining rheometer surfaces with a shear stress that is related to the confining stress by a coefficient of sliding friction. Rearrangements of the grains produce a fluctuating shear stress. In conical geometry, the entire suspension jams. Once jammed, the normal stress in the rheometer maintains the jammed state, even if the angular velocity is reduced far below the DST threshold. In parallel plate geometry suspension near the rheometer axis, where the strain rate is low, does not jam, and may nucleate an unjamming front that unjams the entire suspension with little hysteresis as the rotation rate is reduced.

Surface forces, including both wetting and friction, may explain the DST threshold strain rate $\dot{\gamma}_c$, hysteresis, and the dependence of the rheology on the properties of the solvent. The absence of DST of starch suspensions in nonpolar solvents may be attributed to their lubricity: if it is energetically favorable, compared to dry contact, for grains or grains and confining surfaces to be separated by a thin film of solvent then lubricated flow prevents jamming.

We thank P. Bayly for the use of an AR-G2 (TA Instruments) rheometer, K. Croat, F. Gyngard, S. Handley and A. Nelson for assistance and E. Brown for critical reading and advice. This work was supported in part by American Chemical Society Petroleum Research Fund Grant #51987-ND9.

^a Electronic address: katz@wuphys.wustl.edu

- [1] R. V. Williamson and W. W. Heckert, *Ind. Eng. Chem.* **23**, 667–700 (1931).
- [2] H. Freundlich and H. L. Röder, *Trans. Faraday Soc.* **34**, 308–316 (1938).
- [3] H. A. Barnes, *J. Rheology* **33**(2), 329–366 (1989).
- [4] A. Fall, N. Huang, F. Bertrand, G. Ovarlez and D. Bonn, *Phys. Rev. Lett.* **100**, 018301 (2008).
- [5] A. Fall, F. Bertrand, G. Ovarlez and D. Bonn, *J. Rheol.* **56**, 575 (2012).
- [6] E. Brown and H. M. Jaeger, *Phys. Rev. Lett.* **103**, 086001 (2009).
- [7] E. E. Bischoff White, M. Chellamuthu and J. P. Rothstein, *Rheol. Acta* DOI 10.1007/s00397-009-0415-3 (2009).
- [8] P. Beiersdorfer, D. Layne, E. W. Magee and J. I. Katz, *Phys. Rev. Lett.* **106**, 058301 (2011).
- [9] J. Pryce-Jones, *J. Sci. Instrum.* **18**, 39–48 (1941).
- [10] R. Hoffman, *J. Colloid Interface Sci.* **46**, 491–505 (1974).
- [11] D. A. Head, A. Ajdari and M. E. Cates, *PRL* **64**, 061509 (2001).
- [12] D. Lootens, H. Van Damme and P. Hébraud, *PRL* **90**, 178301 (2003).
- [13] S. von Kann, J. H. Snoeijer and D. van der Meer, *Phys. Rev. E* **87**, 042301 (2013).
- [14] M. Wyart and M. E. Cates, *PRL* **112**, 098302 (2014).
- [15] D. Lootens, H. van Damme, Y. Hémar and P. Hébraud, *Phys. Rev. Lett.* **95**, 268302 (2005).
- [16] E. Brown, *et al.*, *Nature Materials* **9**, 220–224 (2010).
- [17] E. Bertrand, J. Bibette and V. Schmitt, *Physical Review E* **66**, 060401(R) (2002).
- [18] M. E. Cates, J. P. Wittmer, J.-P. Bouchaud and P. Claudin, *Phys. Rev. Lett.* **81**, 1841–1844 (1998).
- [19] P. Hébraud, *Rheol. Acta* **48**, 845 (2009).
- [20] R. J. Larsen, J.-W. Kim, C. F. Zukoski and D. A. Weitz, *Rheol. Acta* **53**, 333 (2014).
- [21] B. Johnson, M. Holland, J. G. Miller and J. I. Katz, *J. Acoust. Soc. Am.* **133**, 1399 (2013).
- [22] E. Brown and H. M. Jaeger, *J. Rheol.* **56**, 875–923 (2012).
- [23] E. Brown and H. M. Jaeger, *Rep. Prog. Phys.*, **77**, 046602 (2014).
- [24] A. B. Metzner and M. Whitlock, *Trans. Soc. Rheol.* **11**, 239–254 (1958).
- [25] C. B. Holmes, M. Fuchs and M. E. Cates, *Europhys. Lett.* **63** (2), 240–246 (2003).
- [26] M. E. Cates, M. D. Haw and C. B. Holmes, *J. Phys.—Condens. Mat.* **17**, S2517 (2005).

- [27] O. Reynolds, *Phil. Mag.* Ser. 5 **20**, 469–481 (1885).
- [28] B. Liu, M. Shelley and J. Zhang, *Phys. Rev. Lett.* **105**, 188301 (2010).
- [29] A. Deboeuf, G. Gauthier, J. Martin, Y. Yurkovetsky and J. F. Morris *Phys. Rev. Lett.* **102**, 108301 (2009).
- [30] R. Hoffman, *Trans. Soc. Rheology* **16**, 155–173 (1972).
- [31] R. Hoffman, *Adv. Colloid Interface Sci.* **17**, 161–184 (1982).
- [32] M. J. Argaud, http://www.scaweb.org/assets/papers/1992_papers/1-SCA1992-08EUR0.pdf (1992).
- [33] C. N. C. Lam, R. Wu, D. Li, M. L. Hair and A. W. Newman, *Adv. Colloid Interface Sci.* **96**, 169 (2002).
- [34] R. Seto, R. Mari, J. F. Morris and M. M. Denn, *Phys. Rev. Lett.* **111**, 218301 (2013).
- [35] *Handbook of Chemistry and Physics* ed. R. C. Weast (Chemical Rubber Company, Cleveland) 48th ed. (1968).
- [36] T. Nakai, S. Sawamura and T. Taniguchi, *J. Mol. Liq.* **65–66**, 365–368 (1995).
- [37] P. Chaikin, Thermodynamics and Hydrodynamics of Hard Spheres: The Role of Gravity, in *Soft and Fragile Matter*, eds. M. R. Evans and M. E. Cates (Taylor & Francis, London) (2000).
- [38] E. Koos and N. Willenbacher *Science* **331**, 897 (2011).